

Drop-on-demand jetting and velocity control of droplet by using the hybrid jetting system

Do-hyung Kim

The Graduate School
Yonsei University
Nanomedical National Core Research Center

Drop-on-demand jetting and velocity control of droplet by using the hybrid jetting system

A master's thesis

**Submitted to the Nanomedical National Core Research Center
and the Graduate School of Yonsei University
in partial fulfillment of the
requirements for the degree of
Master of Science**

Do-Hyung Kim

2011

This certifies that the master's thesis of Do-Hyung Kim is approved.

Thesis Supervisor: Yong-Jun Kim

Jungho Hwang, Thesis Committee Member

Dug Young Kim, Thesis Committee Member

The Graduate School
Yonsei University
January 2011

ACKNOWLEDGEMENT

부족한 제 실력으로 한편의 논문이 완성되는 모습을 보자니 뿌듯함과 함께 부끄러운 마음 역시 밀려옵니다. 마찬가지로 지난 2 년간의 대학원 생활을 마무리하는 시점에서 보람되고 기쁜 기억과 함께 아쉬운 마음 역시 듭니다. 부족한 제가 지난 2 년간의 결실을 맺는 지금 이 자리에 올 수 있도록 도움을 주신 모든 분들께 진심으로 감사의 인사를 드리고자 합니다.

그 어떤 말도 부모님을 향한 감사의 마음을 담기에는 부족해 보입니다. 항상 저를 믿어주시고 자상한 격려를 아끼지 않으신 아버지, 물심양면으로 원조해주신 어머니 감사합니다. 또 타지에 있는 형을 대신하여 가족을 보필하고 있는 의젓한 동생 태형이에게도 심심한 감사의 말을 전합니다.

연구에 대한 깊은 가르침뿐만 아니라 인생의 선배님으로서 많은 배움을 주시고, 부족한 저에게 격려를 아끼지 않으신 김용준 지도교수님께 마음 깊이 감사의 말씀을 올립니다. 좋은 실험 환경을 제공해 주시고, 제 연구의 부족한 점을 세세하게 지도해 주신 황정호 교수님과 따뜻한 격려와 함께 몸소 연구자로서의 길을 보여 주신 김덕영 교수님께 감사드립니다.

연구뿐만 아니라 사회생활과 인간관계에 대하여 깊은 연륜으로 가르침을 주시고, 골프 입문의 기회마저도 열어주신 영재 형 감사드립니다. 연구실에서 함께한 기간이 짧아 아쉬웠지만 다행히도 사회에서 많은 시간을 함께 하게 될 용호 형과 은수 형께도 진심으로 감사드립니다. 지난 2 년 동안 술을 벗 삼아 때론 다정하고 때론 따끔한 충고를 아끼지 않으신 연구실의 중심,

승일이 형 감사합니다. 앞으로 연구실의 든든한 리더가 되어 주실 혜경 누나, 다재다능한 순명이형, 힘들 때마다 힘이 되어주신 재영이형, 연구에 대한 열정을 되새겨 주신 준성이형께 감사 인사드립니다.

2년 동안 심심할 겨를이 없게 해준 동네 친구 충일이, 나를 많이 괴롭혔지만 밋지 않은 친구 병근이, 음식뿐만 아니라 학문에도 대식가인 성은이, 패션리더이자 큰 비상을 위하여 살짝 움츠렸던 홍래, 함께 하는 시간이 더 많았다면 좋았을 것 같은 코드가 잘 맞는 동생 민구, 혼돈의 세계에서 즐거운 시간을 함께 보낸 내 동기 석영이, 동생이지만 배울 점이 많은 도시남자 용환이, 나의 옆자리에서 연구실 후배이자 좋은 친구가 되어준 듬직한 명수, 연구에 대한 열의가 넘쳐서 앞으로가 기대되는 동현이, 훌륭한 도시 대구 출신의 착하고 똑똑한 후배 혜린이, 제 연구를 이어가게 될 성실한 상면이에게 감사의 마음을 전합니다. 그리고 연구에 매진할 수 있도록 도와주시고, 옆에서 어머니와 같은 버팀목이 되어 주신 성지 이모께 역시 깊은 감사의 말씀을 드립니다. 마지막으로 지난 대학원 시절 동안 제 곁을 지키며 큰 활력과 안식처가 되어준 상록양에게 따뜻한 마음을 전합니다. 또한, 비록 언급 드리지 못했더라도 그 동안 제 곁에서 추억을 함께 한 소중한 분들께 진심으로 감사드립니다.

대학원 생활이 어느덧 종점을 향하고 있습니다. 연구적으로 얻은 많은 배움뿐만 아니라 그 이상으로 값진 것은 함께 울고 웃으며 때론 힘들기도 한 대학원 시절의 든든한 동반자이자 지원군이 되어준 연구실 가족들을 알게 된 것이 아닐까 생각해봅니다. 연구실에서 쌓은 밑거름을 토대로 사회에

나가서도 MEMS 연구실에 부끄럽지 않은 사회인이 되도록 노력할 것을 약속드립니다.

사람이 얼마나 행복한 가는 그의 감사의 깊이에 달려있다고 하던가요. 마음 깊이 진심으로 감사할 수 있는 여러분이 있기에 저는 정말 행복한 사람입니다.

2011 년 1 월

김도형

TABLE OF CONTENTS

LIST OF TABLES	ix
LIST OF FIGURES	x
ABSTRACT	xii

CHAPTER

I. INTRODUCTION	1
1.1 Motivation	1
1.2 Direct write technology	4
1.3 Back ground	7
1.3.1 Inkjet printing	7
1.3.2 History of cone-jet mode of EHD printing	11
1.3.3 Research trend	14
1.4 Outline	18
II. PRINCIPLE & DESIGN	19
2.1 Principle of EHD jet printing	19
2.2 Ring extractors integrated hybrid jetting system (HJS)	22
2.2.1 Principle of ring extractors integrated HJS	22
2.2.2 Design	24
2.2.3 Simulation	26

2.3. Thermal bubble hybrid jetting system (HJS)	27
2.3.1 Principle of thermal bubble HJS	27
2.3.2 Design & fabrication	29
III. EXPERIMENT AND RESULTS	31
3.1 Ring extractors integrated HJS	31
3.1.1 Experimental setup	31
3.1.2 Drop-on-demand jetting	33
3.1.3 Velocity control of droplets	37
3.2 Thermal bubble hybrid jetting system	44
3.2.1 Experimental setup	44
3.2.2 Jetting results of fabricated thermal jet head	46
IV. Conclusion	47
4.1 Summary	47
REFERENCE	49

List of Tables

Table 2.1 : the characteristics of the ring extractors.

Table 3.1 : Physical properties of the liquid used in the ring extractors integrated HJS

Table 3.2 : The distance between the glass capillary and tip of droplets.

Table 3.3 : Physical properties of the liquid used in the thermal bubble HJS.

List of Figure

- Figure 1.1 : Comparisons of Optical Lithography & DW Technologies
- Figure 1.2 : Direct printing process parameter comparisons
- Figure 1.3 : Piezoelectric pressure induced ink droplet ejection
- Figure 1.4 : Principle of thermal bubble printing
- Figure 1.5 : Different regions of cone-jet mode
- Figure 1.6 : Schematic forces in the liquid cone
- Figure 1.7 : Experimental setup of electrohydrodynamic jet printing
- Figure 1.8 : Results of electrohydrodynamic jet printing added ring-shaped electrode, rectangular shape inductor, curved-shape inductor, symbol of YONSEI
- Figure 1.9 : Experimental setup of DOD (drop on demand) printing
- Figure 1.10 : Meniscus shape change according to applied pulse voltage
- Figure 1.11 : Applied voltage change according to distance between capillaries
- Figure 2.1 : Schematic of electrospray
- Figure 2.2 : Mode of electrospray
- Figure 2.3 : Principle of ring extractors integrated HJS
- Figure 2.4 : The driving waveform of the piezoelectric actuator
- Figure 2.5 : Schematic of designed ring extractors
- Figure 2.6 : Electric field analysis of (a) pin electrode and (b) ring extractors
- Figure 2.7 : Principle of thermal bubble HJS
- Figure 2.8 : Driving waveform of thermal bubble HJS
- Figure 2.9 : Fabrication steps of the thermal bubble HJS

Figure 2.10 : Fabricated thermal jet head and PCB nozzle

Figure 3.1 : Experimental setup of ring extractors integrated HJS.

Figure 3.2 : Detail meniscus control through a piezoelectric actuator. Pulsation continued until 150 μs after the waveform applied.

Figure 3.3 : DOD ejection results using the proposed HPS. The Jetting cycle and droplet volume were under 100 μs and 1.33pl.

Figure 3.4 : Jetting results of various driving waveform at (b) 100 μs and (c) 300 μs

Figure 3.5 : The jetting of droplet in the electrostatic field that is applied by the ring extractors

FIGURE 3.6 : Velocity control of droplets using the ring extractors integrated HJS. (a) jetting characteristic in the electrostatic field, jetting results of various DC voltage at (b) 100 μs and (b) 300 μs , and

Figure 3.7 : The average velocity (v_{droplet}) of the droplets between 100 μs and 300 μs in varying supplied DC voltages

Figure 3.8 : Experimental setup of thermal bubble HJS.

Figure 3.9 : Drop-on-demand jetting result of the fabricated thermal jet head.

ABSTRACT

Drop-on-demand jetting and velocity control of droplets by hybrid jetting system

Do-Hyung Kim

School of Mechanical Engineering

The Graduate School

Yonsei University

Direct write techniques have been widely studied because it is a low-cost, high-speed, and environmentally-friendly manufacturing process. The technique is based on ink-jet or EHD. The ink-jet printing method can make droplets with high jetting-frequency(10-100 kHz), while the droplet size is limited to become larger than the nozzle size. On the contrary to this, the EHD printing method can makes droplets ten-times smaller than the nozzle size, but the jetting-frequency is limited due to time delay for Taylor-Cone formation. In order to generate ultra fine droplets with high-throughput, a technical convergence of ink-jet and EHD methods is required. And also, to realize multi-nozzle jetting systems, a control technique of drop-velocity from each nozzle is required.

In this paper, we developed two types of hybrid printing system which are ring

extractors integrated hybrid jetting system and thermal bubble hybrid jetting system.

Ring extractors integrated hybrid jetting system (HJS) that solves the problems of pin electrode of previous HJS. By using this system, ultra fine droplets (1.33pl) were generated with short jetting cycle at relatively low DC voltage (2.3kV), in comparison with previous HJS (~5kV). In addition, in order to control the droplet velocity, we tested jetting performance for various DC voltages of ring extractors at fixed driving waveform. As a result, the drop velocity could be controlled by tuning the applied DC voltage to the HPS. It can contribute to reduce velocity deviation of droplets in multi-nozzle jetting systems without changing volume of droplets.

For multi nozzle HJS, we made thermal inkjet head. By using PCB nozzle, we improved the electrical insulating properties of nozzle surface and reduced fabrication cost. Using these multi nozzle hybrid jetting head, we could control the meniscus and eject droplets with frequency of 500Hz.

CHAPTER I

INTRODUCTION

1.1 Motivation

Low cost, high speed and environmentally friendly process are advantages of the direct write techniques because they directly form micro- to nano scale patterns without the photolithographic process [1]. So, direct write techniques have been widely studied using various printing methods for realizing fine patterns.

In the direct write techniques, there is an inkjet printing technology. This technology is non contact, three-dimensional manufacturing, and an on-demand method. So, it was previously applied in bio-applications [2] and electronics [3]. This technology is divided into a thermal bubble type [4] and piezoelectric type [5] according to the droplet generation method. Each method makes a droplet using piezoelectric material or heater material that is well known as a reliable material. Therefore, droplet control for DOD (drop-on-demand) with high jetting frequency (10~100kHz) is easy. However, in ink-jet printing, the droplet size is usually larger than the nozzle diameter [6]. So, for realizing fine patterns, reducing the nozzle size is required, making it a difficult fabrication with high cost. And Miniature nozzles are susceptible to plugging and breaking when the high viscosity ink is used [7]. Because of these problems, recently, the electrohydrodynamic (EHD) printing has been studied. For the DOD jetting, pulsed voltage or lower DC voltage than that of the cone-jet mode is used in EHD printing [8].

This method can create fine droplets smaller than the nozzle size because the droplets are ejected at the apex of a liquid cone [9]. However, the on-demand jetting frequency is limited due to the time delay for meniscus formation [10]. Thus, the jetting frequency is much lower than that of ink jet printing method such as thermal bubble and piezoelectric methods.

Recently, research about the hybrid jetting system (HJS) that uses both an EHD printing method and mechanical actuation was presented for jetting fine droplets with a high jetting frequency [11]. In this system, a pin electrode was used to apply the EHD force. It was located under the substrate where ink is evaporated. So, there is an electric field distortion and interference phenomenon depending on the quality of the material and thickness difference of the substrate. Usually, in EHD printing, fine droplet formation and regular mode of jetting are easy to achieve when the positive excitation voltage is applied to the capillary [12]. However, in this system, a positive excitation voltage was applied to the pin electrode located under the substrate. So, it needed high dc voltage ($\sim 5\text{kV}$) for electrohydrodynamic jetting.

In the multi nozzle piezoelectric printing, there is deviation in the velocity of droplets between nozzles due to the surface conditions of the nozzle plates, ink filling states within the chamber and fabrication errors of the head, and so on [13]. It should be reduced for detailed and equal pattern formation. To reduce the velocity deviation of the nozzles, previous studies have aimed to drive the waveform of a piezoelectric actuator. However, the change of driving waveform leads to a change of droplet size as well as velocity change of droplet [14]. However, in the latter technique, it is very difficult to precisely control the driving waveform. So, realizing a printing technique that can control the velocity of droplets at a fixed driving waveform is necessary.

To overcome the above mentioned limitation of pin electrode in the hybrid jetting system (HJS) and velocity deviation of droplets in the multi nozzle printing, we developed ring extractors integrated HJS. To demonstrate the ring extractors, electric field analysis was performed. This system offers a jetting of ultra fine droplets with high jetting frequency and controls the droplet velocity without changing volume at a fixed waveform.

And, to improve throughput of hybrid jetting system, we developed thermal inkjet head for applying hybrid jetting system (T-HJS). This thermal inkjet head was made by PCB process and MEMS process. It made by simple fabrication skill without DRIE technique that is usually used for making the thermal jet head. To enhance the electrical insulating properties, nozzle was made by PCB process. In these multi nozzle hybrid jetting system, we could control the meniscus and eject droplets with frequency of 500Hz. The liquid used in this study was 99.7% C_2H_5OH

1.2 Direct write technology

Various electronic devices, including portable devices are becoming smaller and more complicated, micro/nano scale has increased interest in printing. Direct write technology is the most recent and novel approaches of forming a fine pattern whose line width ranges from the meso to the nanoscales. The existing semiconductor production process requires expensive photomasks, exposures and the process like sputtering that has low efficiency in material uses. During the last few years of process renovation, cost reduction reached to its limit in these processes. As well as rising of the environment problem caused by chemicals like acids used during the process. To solve these problems, direct write technology that can form a micro pattern from a nanometer size to few micrometers is being researched briskly to replace the existing semiconductor production process. Figure 1.1 shows a comparison of printing and traditional lithography technology. The direct write technology can acquire a pattern or a structure by deposition of ink, which has characteristics like little wastes of materials, reduction on production cost, fast production, and environmentally-friendly process. Also, acquiring the pattern through spray makes making of two or three dimension structures possible, and gives an advantage to scaling-up. Figure 1.2 shows some direct printing processes parameter comparison. An advantage of ink-jet printing technology, which is the most representative method of direct write technology, is the creation of a droplet smaller than 50pL by one-by-one forming method. In recent years, Ink-jet printing has been receiving growing interest as a method to deposit functional materials, as opposed to the more conventional graphics applications. Ink-jet printing is particularly good for the deposition of small amount of materials that have specific

electrical, optical, chemical, biological, or structural functionalities onto well defined locations on a substrate. The materials deposited can be soluble liquids, dispersions of small particles, melts or blends. However, this ink-jet printing has a size of discharging droplet that is larger than nozzle size, which means making a 10um wide line requires the nozzle that is smaller than 5.3um. If the functional nanocolloid solution formed with nano particle powder, liquid, and dispersing agent is used on a miniature nozzle, the nozzle will be clogged. Also, productivity of the nozzle drops as the width of nozzle gets narrower. To overcome these issues, electrohydrodynamic jet printing is being researched actively, and this method uses electrical power in addition. For that reason, the size of discharged jet is 1/20 of width of the nozzle, so relatively larger nozzle can be used.

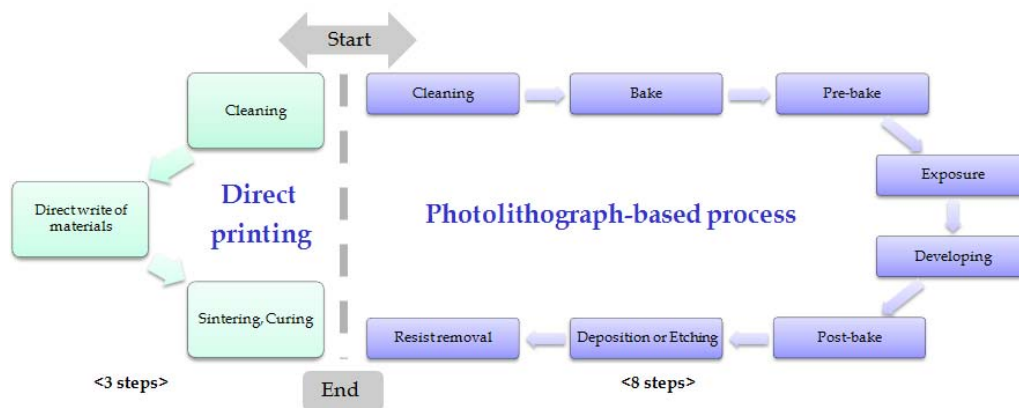


Figure 1.1 Comparisons of Optical Lithography & DW Technologies

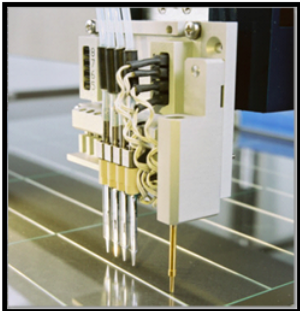



				
Ink jet printing	Screen printing	Gravure printing	Offset printing	
Line width	• 20 μ m	70 μ m	80 μ m	20 μ m
Viscosity	• 1~30cps	500cps~	50~200cps	40000cps~
Frequency	• 20kHz	X	X	X
Characteristics	• Contactless	Contact	Contact, Mold	전촉식, Mold

Figure 1.2 Direct printing process parameter comparisons

1.3 Back ground

1.3.1 Inkjet printing

1.3.1.1 Piezoelectric printing

The basic principle of piezoelectric drop-on-demand inkjet technology is the ejection of fluid droplets from nozzles, termed a print head, by a pressure wave created by the actuation of piezoelectric material, on the application of voltage pulses. Suitably bonding the piezoelectric actuator to an ink-filled cavity, results in an expansion or contraction in the cavity volume due to the mechanical displacement of the piezoelectric, creating a pressure wave in the ink. This pressure wave travels through the fluid into the nozzle bore resulting in the ejection of a specific column of fluid. Due to pressure wave reversal at the nozzle, after the drive pulse has completed the pulse cycle, the fluid in the nozzle bore begins to retract whilst the ejected fluid column travels away from the nozzle with a specific momentum, dictated by the kinetic energy of the droplet. Under optimum conditions the result of this action is the separation of a fluid packet, which possess a detachment tail (ligament) and that subsequently forms a drop due to surface tension effects providing that the spacing between the nozzle and the substrate surface is large enough. The velocity of the ejected drop is directly related to the kinetic energy induced in the drop by the pulsed pressure wave. This process is depicted in Figure 1.3. The most commonly used piezoelectric material in print head manufacture is PZT (lead, zirconate titanate)

ceramic, which can be employed in a number of operating modes. Bend, push and shear design principles have been successfully implemented in many commercially available print heads. During manufacture, the PZT is poled and then electrodes are placed on the surface of the PZT. In both the bend- and push-mode designs, the electric field generated between the electrodes is in parallel with the polarization of the PZT. In practical implementation, a thin diaphragm between the PZT and ink is incorporated to prevent interactions between them. In shear-mode, however, the electric field is applied perpendicular to the polarization of the poled PZT employing interdigitated or planar electrode configurations. The shear action deforms the PZT against ink to eject the droplets. In this case, the PZT becomes an active wall in the ink chamber and interaction between ink and PZT is an important aspect of a shear-mode print head design.

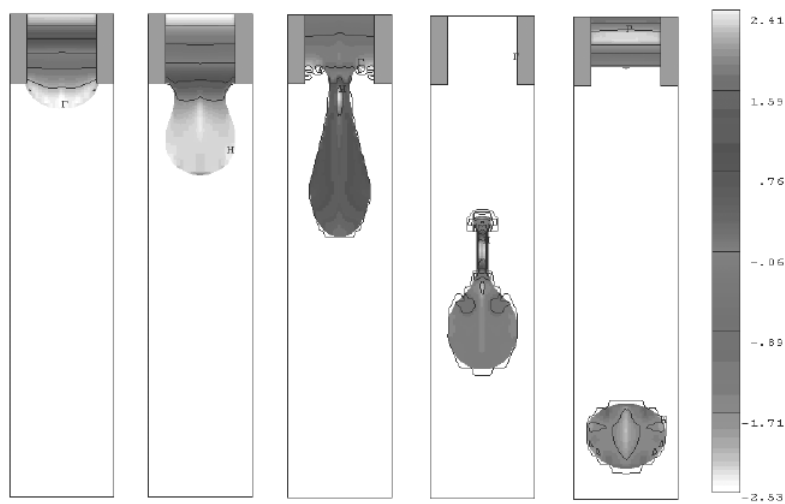


Figure 1.3 Piezoelectric pressure induced ink droplet ejection

1.3.1.1 Thermal bubble printing

The most common inkjet technology is called *thermal* because it uses heat inside its print head to boil a tiny quantity of water based ink. Boiling produces tiny bubbles of steam that can balloon out from the nozzle orifices of the print head. The thermal mechanism carefully controls the bubble formation. It can hold the temperature in the nozzle at just the right point to keep the ink bubble from bursting. Then, when it needs to make a dot on the paper, the print head warms the nozzle, the bubble bursts, and the ink sprays from the nozzle to the paper to make a dot [Figure 1.4]. Because the bubbles are so tiny, little heat or time is required to make and burst the bubbles; the print head can do it hundreds of times in a second.

This obscure process was discovered by a research specialist at Canon way back in 1977, but developing it into a practical printer took about seven years. The first mass marketed PC inkjet printer was the Hewlett-Packard ThinkJet, introduced in May 1984, that used the thermal inkjet process (which HP traces back to a 1979 discovery by HP researcher John Vaught). This single-color printer delivered 96 dot per inch resolution at a speed of 150 characters per second, about on a par with the impact dot matrix printers available at the same time. The technology-not to mention speed and resolution-have improved substantially since then. The proprietary name *BubbleJet* used by Canon for its inkjet printer derives from this technology, although thermal bubble design is also used in printers manufactured by DEC, Hewlett-Packard, Lexmark, and Texas Instruments

The heat that makes the bubbles is the primary disadvantage of the thermal inkjet system. It slowly wears out the print head, requiring that you periodically replace it to

keep the printer working at its best. Some manufacturers minimize this problem by combining their printers' nozzles with their ink cartridges so that when you add more ink you automatically replace the nozzles. With this design you never have to replace the nozzles, at least independently, because you do it every time you add more ink.

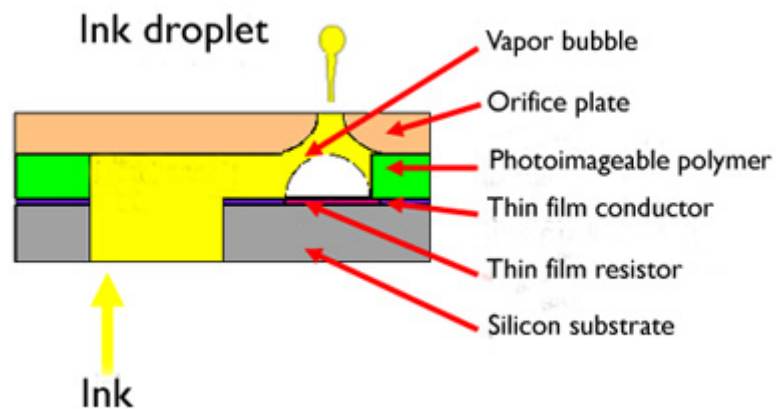


Figure 1.4 Principle of thermal bubble printing

1.3.2 History of cone-jet mode of EHD printing

Electrohydrodynamic atomization in the cone-jet mode has been studied for many years. The phenomenon was first mentioned in ‘De Magnete’ by William Gilbert in 1600. He observed that a piece of amber, held at a suitable distance, attracts spherical droplets lying on a dry surface, and draws them up into cones. However, it was Zeleny (1914, 1915, 1917), who gave the first solid scientific description of the process. After Vonnegut and Neubauer (1952) rediscovered this phenomenon, many people have contributed to the understanding of Electrohydrodynamic atomization in the cone-jet mode.

Electrohydrodynamic atomization in the cone-jet mode has to be described by at least five different regions. Figure 1.5 shows the five different regions. The first process, which has region I and region II, is the acceleration of the liquid in the liquid cone. Based on the work of Gañán-Calvo et al. (1997), Fernández de la Mora and Loscertales (1994), and many other people, the following description of this acceleration can be given. The electric field induces a free surface charge in the cone surface. In a liquid, charge is mainly transported by ions. So, the free charge at the liquid surface mainly consists of ions. Due to this surface charge, the normal electric field inside the liquid is small compared to the normal field outside the liquid. This acceleration process and the shape of the liquid cone are a result of the balance of the liquid pressure, liquid surface tension, gravity and electric stresses in the liquid surface, and of the inertia and viscosity of the liquid. Figure 1.6 shows the processes that play a role in the liquid cone. Taylor (1964) was the first to describe the balance between the surface tension stress and the normal electrical stress in a liquid cone.

The second process, which has region III and region IV, is the break-up of the jet into

droplets. The jet emerging at the cone apex breaks often up into a bimodal size distribution. This bimodal size distribution occurs because the jet breaks up into main droplet with a narrow size distribution, and a number of smaller secondary droplets. The break-up of a jet has been studied by many people. For instance, Rayleigh (1878) and Weber (1931) have presented theories to predict the growth rate of varicose instabilities on a liquid jet.

The third process is deposition mechanism of liquid jet in electrohydrodynamic printing. This mechanism of process tries to study and research at present. The special feature and characteristic of cone-jet mode of electrohydrodynamic spraying have attracted many researchers. Taylor calculated analytically a conical shape, which balanced the surface tension and the electrical normal stress with an inviscid liquid. Fernández et al. (1990) provided scaling laws for jet diameter based on dimensional analysis of all parameters involved in the electrohydrodynamic spraying. Gañán-Calvo (1997) provided scaling law for the generated droplet size and compared with the experimental results. Chen and Pui (1997) generated with liquids of different relative permittivity and compared the scaling laws with their results. Hartman et al. (1999, 2000) studied the break-up phenomenon of electrically driven liquid jet and developed the Calvo's scaling laws.

Hak Fei Poon (2002) studied the calculate equation of Jet length before the breakup of jet. Li (2006) investigated the spraying phenomenon with pulse bias voltages and Chen et al. (2006) provided scaling laws for drop formation under pulse electrohydrodynamic spraying.

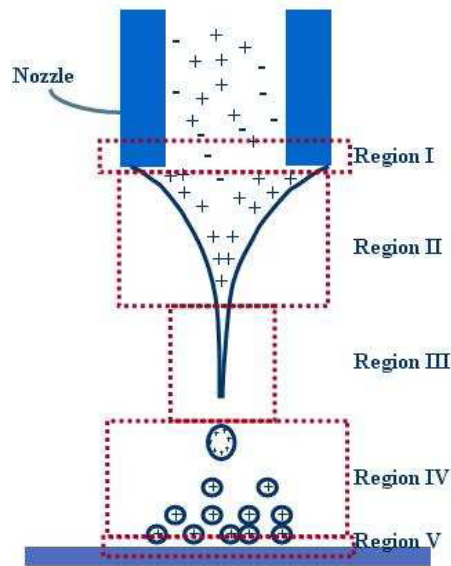


Figure 1.5 Different regions of cone-jet mode

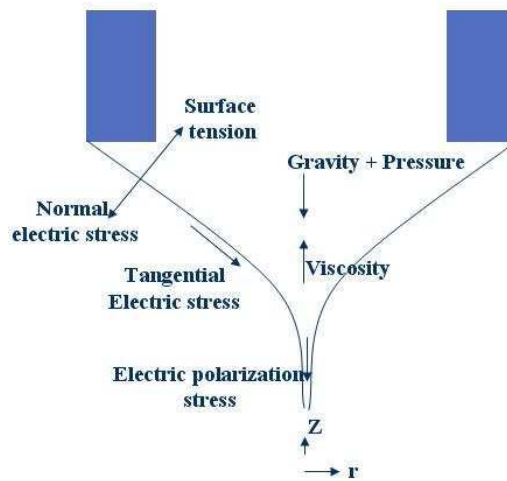


Figure 1.6 Schematic forces in the liquid cone

1.3.3 Research trend

1.3.3.1 Continuous jet printing with focusing device

Previous research in EHD was conducted using pin-shaped nozzle. In case of pinshaped nozzle, the contact area where between nozzle and ink was small. It makes wetting phenomenon that nozzle wall wetted by ink. Wetting phenomenon obstructs stability of cone-jet mode. If the cone-jet is not stable state, it makes positioning error of the printed pattern. It must be solved for fine patterning. D. Y. Lee tried to get ability of cone-jet. He was use of ring-shaped second electrode which makes convergence of electric field. Ring-shaped electrode located between nozzle and substrate. When the cone-jet ejected from tip of meniscus, ringshaped electrode helps that jet arrives to selected position. Figure 1.7 shows experimental system. And Fig. 1.8 shows the results of experiment. The nozzle and second electrode applied positive voltage and negative voltage applied to pin-shaped ground electrode [15]. In this experimental, the stability of cone-jet was achieved. But, the ground electrode still located under substrate, stable printing is impossible like previous researches. Because the ground electrode located under substrate, printing process is influenced by characteristics of substrate.

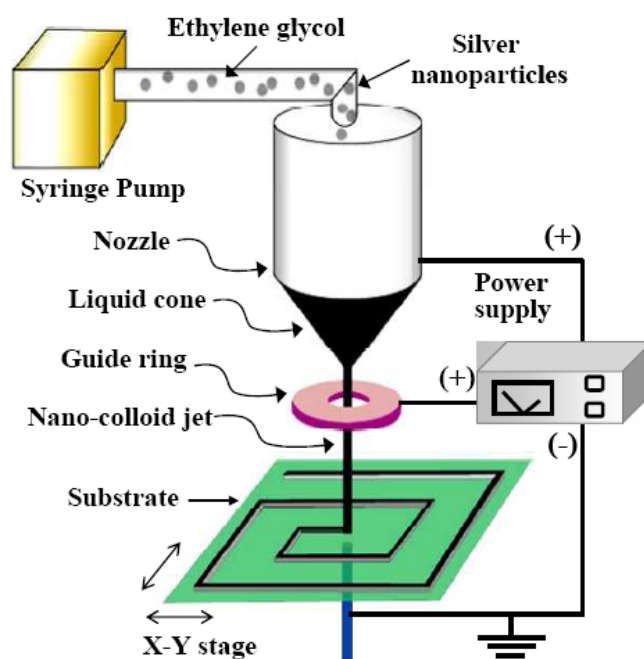


Figure 1.7 Experimental setup of electrohydrodynamic jet printing

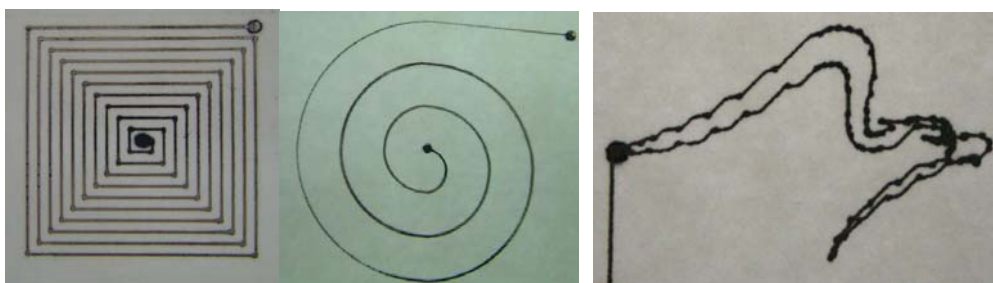


Figure 1.8 Results of electrohydrodynamic jet printing added ring-shaped electrode, rectangular shape inductor, curved-shape inductor, symbol of YONSEI

1.3.3.2 DOD (drop on place) using pulse voltage

One of method in EHD is DOD (drop on demand). In order to selective printing, each nozzle which contained in multi-nozzle must be controlled. In case of DOD, most researcher uses pulse voltage. Li has been tried to eject droplet from tip of meniscus using bias voltage plus pulse voltage [16]. Figure 1.9 shows the experimental setup of DOD printing. It has two kinds of power supply. One thing is for bias voltage supplying and the other thing is for pulse voltage supplying. Figure 1.10 shows the changing of meniscus shape according to applied pulse voltage. When the pulse voltage applied to nozzle during bias voltage activated, meniscus is extended. And then, droplet is ejected from tip of meniscus. However, there are some limitations. First, ejected droplet is not exact droplet which means droplet is defined as broken jet. Second, according to Regele, when the pin-shaped single nozzle is arrayed, operating voltage is changed according to distance from nozzle to nozzle as shown in Fig. 1.11 [17]. It implies that pin-shaped nozzle arrays were needed wide range of applied voltage for controlling each nozzle. Therefore, pin-shaped nozzle is hard to apply to multi-nozzle. Because, operating nozzle is changed in multi-nozzle. It makes various distance between nozzles. Consequently, each nozzle does not controllable using constant voltage. If we want to make multi-nozzle, the problem must be solved.

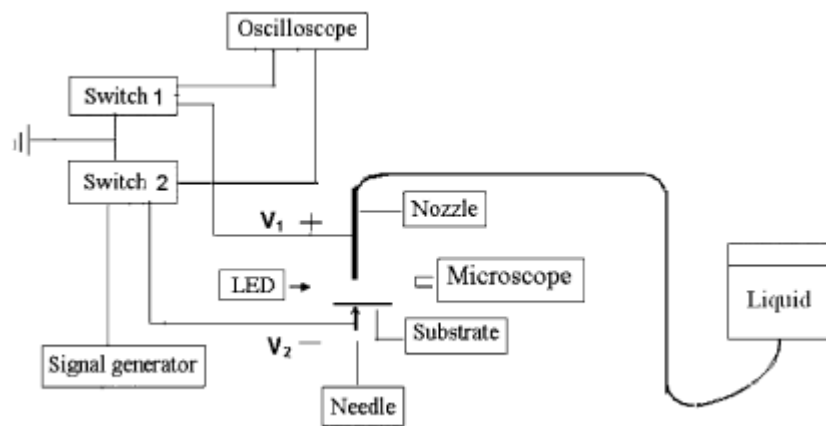


Figure 1.9 Experimental setup of DOD (drop on demand) printing



Figure 1.10 Meniscus shape change according to applied pulse voltage

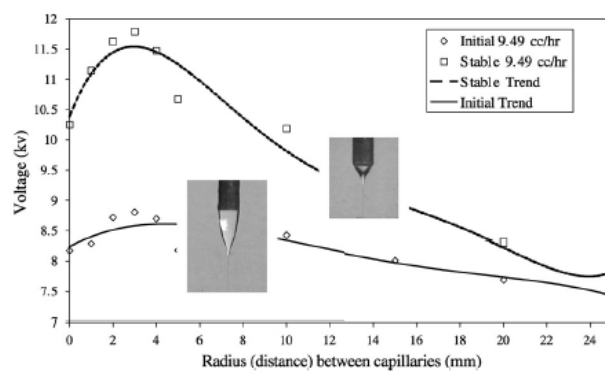


Figure 1.11 Applied voltage change according to distance between capillaries

1.4 Outline

In this research, design, fabrication and characterization of hybrid jetting system(HJS) were introduced. Two types of hybrid jetting system which are ring extractor integrated hybrid jetting system with piezoelectric actuation and thermal bubble hybrid jetting system were demonstrated for ultra fine droplets with high jetting frequency.

In ring extractors integrated hybrid jetting system, ring extractors for stable jetting and controlling the droplet velocity were fabricated. And electric field generation of ring extractors was demonstrated by using simulation tool (Maxwell 3D.). In this system, ultra fine droplets generation is possible. And control of droplet velocity is possible without changing droplet volume.

For multi nozzle HJS, we made thermal inkjet head. By using PCB nozzle, we improved the electrical insulating properties of nozzle surface and reduced fabrication cost. Using these multi nozzle hybrid jetting head, we could control the meniscus and eject droplets with frequency of 500Hz.

Chapter 2 will describe principle and design of two types of hybrid jetting system.

In chapter 3, the results of ring extractors integrated HJS and thermal bubble HJS are described.

In chapter 4, the conclusion of total experimental results will be discussed.

II. PRINCIPLE & DESIGN

2.1 Principle of EHD jet printing

Electrospraying (electrohydrodynamic spraying) of liquids is a physical process caused by the electric force applied to the surface of a liquid. The droplets generated by the electrospray method have electrical charge, usually a few magnitudes greater than elementary charge that changes their electrospray properties, like for example electrical mobility. In general, the size of drops produced depends on the applied voltage, surface tension, electrode size and configuration, liquid flow rate, and electrical properties of the liquid, such as dielectric constant and electrical conductivity.

A variety of spraying modes have been reported as shown in Fig. 2.1. One of the most interesting modes is the cone-jet mode, often referred to as the Taylor Cone, in which the meniscus forms a cone extended at its apex by a permanent jet whose breakup gives rise to the droplets. When an external electric field is applied to a solution, ions in the solution will aggregate around the electrode of opposite polarity. Positive ions travel to the negatively charged electrode and negative ions travel toward the positive electrode. For example, when a positive (+) voltage is applied to the multi-nozzle, the ions in the solution of like polarity will be forced to aggregate at the surface charge will cause the drop to distort into the shape of a cone. If the electric potential of the surface charge exceeds a critical value, the electrostatic forces will overcome the solution surface tension. A thin jet of solution will erupt from the

surface of the cone and travel toward the nearest electrode of opposite polarity, or electrical ground (Taylor, 1964) .

The first theoretical analysis of this phenomenon is due to Rayleigh who showed that radial direct forces from interfacial charge counteracted the surface tension of the drop (Rayleigh, 1882). Zeleny (1914) made the first observation of what is now known as the cone-jet transition. Taylor (1964 and 1969) first proposed the static balance condition between surface tension and electrical stress on a spherical surface to obtain the jet.

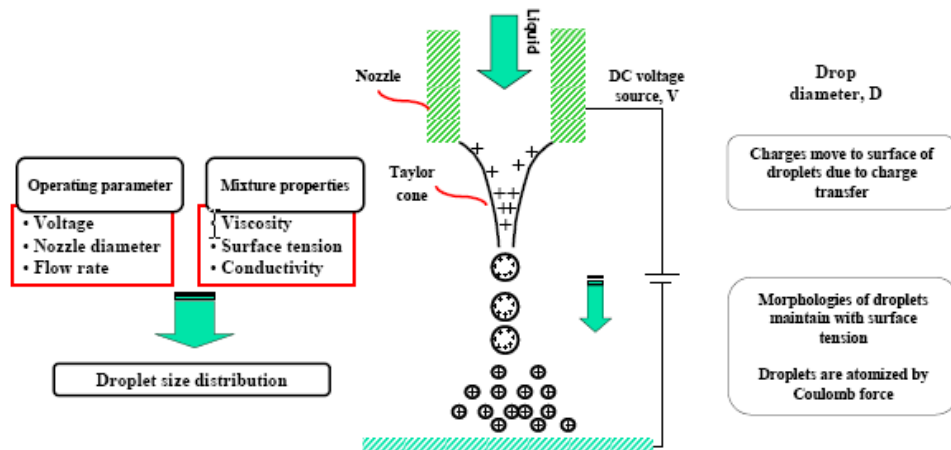


Figure 2.1 Schematic of electrospray

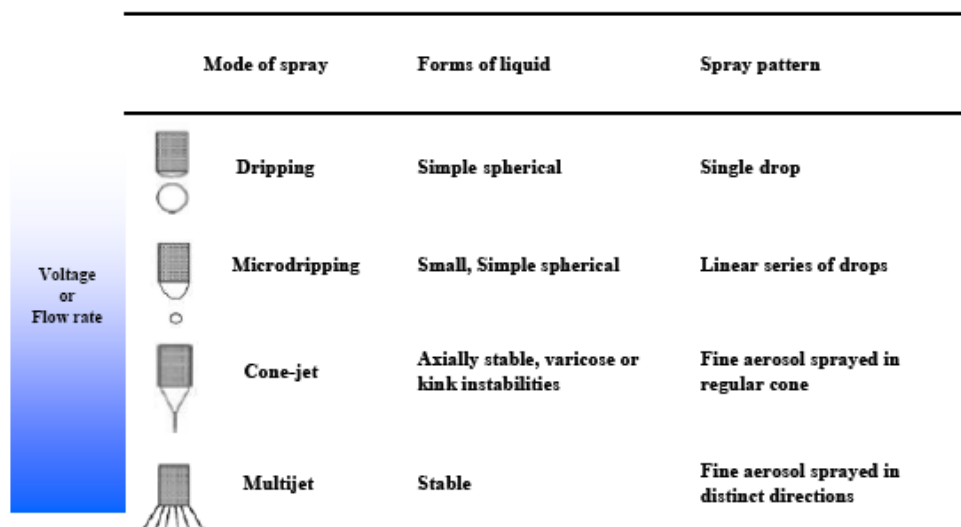


Figure 2.2 Mode of electro spray

2.2 Ring extractors integrated hybrid jetting system (HJS)

2.2.1 Principle of ring extractors integrated HJS

Figure 2.3 shows the principle of operation of the Ring extractors integrated HJS. In this system, the capillary is equipped with a piezoelectric actuator for on-demand jetting. When a driving waveform (detailed in figure 2.4) is applied to the piezoelectric actuator, the wall of the capillary deforms, and the pressure inside the capillary increases. Such a high pressure allows the extrusion of the liquid meniscus outside of the capillary. Here, it is important to optimize the applied driving waveform and the back-pressure in accordance with the kind of liquid because large droplets are ejected by the excessive displacement of the piezoelectric actuator. When the liquid meniscus is deformed and extruded outside of the capillary, EHD jetting is initiated because the electric potential on the surface of the meniscus exceeds a critical value due to the high voltage that is applied between the capillary and Ring extractors. When the driving waveform is turned off and the pressure inside the capillary is decreased, the meniscus of the liquid returns to the initial position. Then, one cycle of the jetting is complete.

In contrast to the pulsed cone-jet mode (where the operational voltage is several kV), the shape of the liquid meniscus can be controlled through a piezoelectric actuator that is operated by an electric potential of tens of volts. Using this principle, ultra-fine droplets can be generated with a high frequency of up to 1 kHz. Furthermore, the response characteristics of the HJS are better than those of the pulsed cone-jet and pulsating jet modes because the delay time for making a Taylor cone is negligibly small.

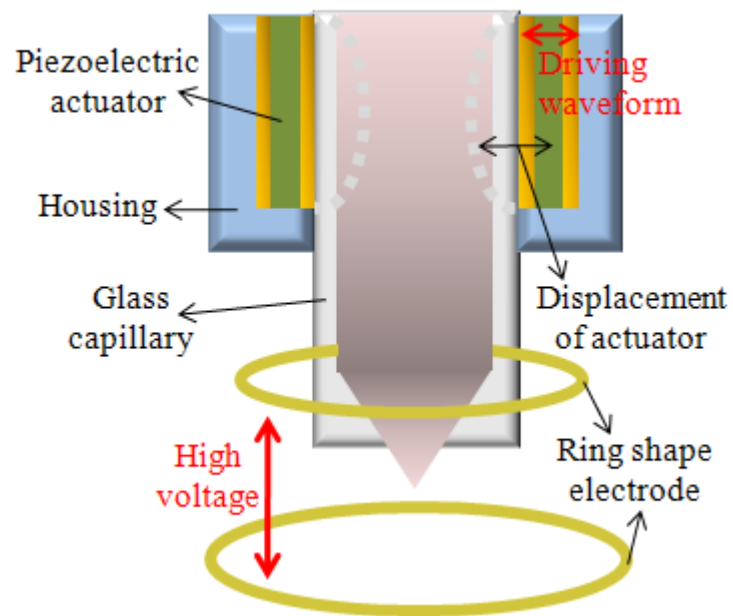


Figure 2.3 Principle of ring extractors integrated HJS

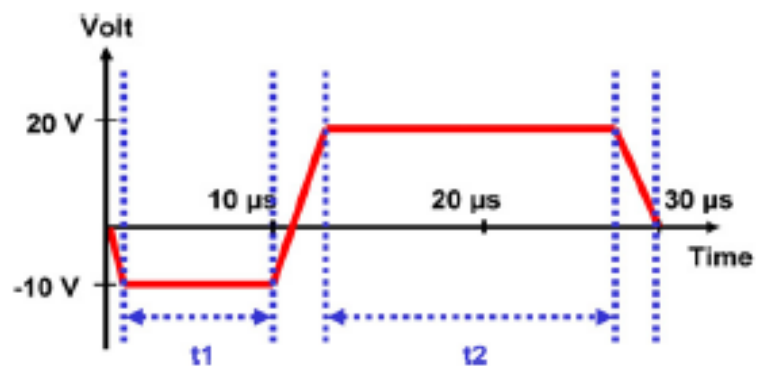


Figure 2.4 The driving waveform of the piezoelectric actuator

2.2.2 Design

Figure 2.5 shows the schematic view of the print head of the proposed ring extractors integrated HJS. It is composed of a piezoelectric actuating head and ring extractors and acrylic.

The piezoelectric actuating head consists of a piezoelectric actuator and a glass capillary. The inner and outer diameters of the glass capillary are 60 μm and 300 μm , respectively. The ring extractors consist of an upper ring electrode and a bottom ring electrode. They are fabricated by a PCB process to secure insulation between the piezoelectric actuator and electrode of ring extractors. By using ring extractors, the EHD force application is available without considering the kinds and conditions of a substrate, and the stable EHD force application between each the nozzle is possible in the case of multiple nozzles.

For EHD printing using the glass capillary, a difficult technique is required to form electrode inside the glass capillary such as Pt wire [18] or aluminum pole [19]. However, it can apply the EHD force without inner electrode of glass capillary. The acrylic jig fastens a piezoelectric actuating nozzle with the ring extractors.

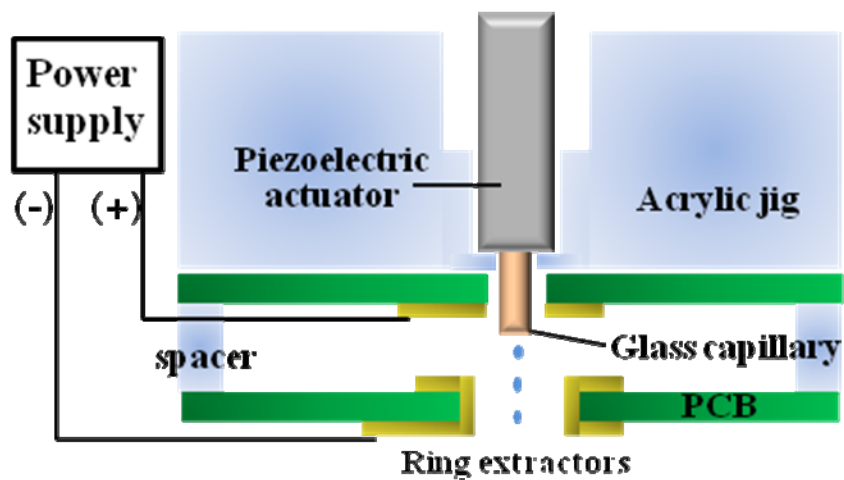


Figure 2.5 Schematic of designed ring extractors

Nozzle size	60 μm	Thickness of PCB	0.6 mm
Distance of extractors	2 mm	Thickness of electrode	30 μm
Size of upper ring electrode	1.2 mm	Size of bottom ring electrode	3 mm

Table 2.1 the characteristics of the ring extractors.

2.2.3 Simulation results

Figure 2.6 shows a comparison of the electric field analysis in (a) a previous pin electrode type [11] and (b) proposed ring extractors type. The same electric voltage (5kV) was applied in each type.

When the electric voltage is applied to the pin electrode, the electric field is strongly formed on the electrode below the substrate [Fig. 2.6(a)]. So, it could not apply enough electrostatic force to efficiently eject the droplets to the nozzle. When the electric voltage is applied to the upper ring electrode of ring the extractors, we could confirm that the electric field is strongly formed within the upper ring electrode and bottom ring electrode [Fig. 2.6(b)]. Therefore, the ring extractor type can create the jetting of ultra fine droplets at relatively low DC voltage (2.3 kV), in comparison with the pin electrode of the previous HJS (~5kV).

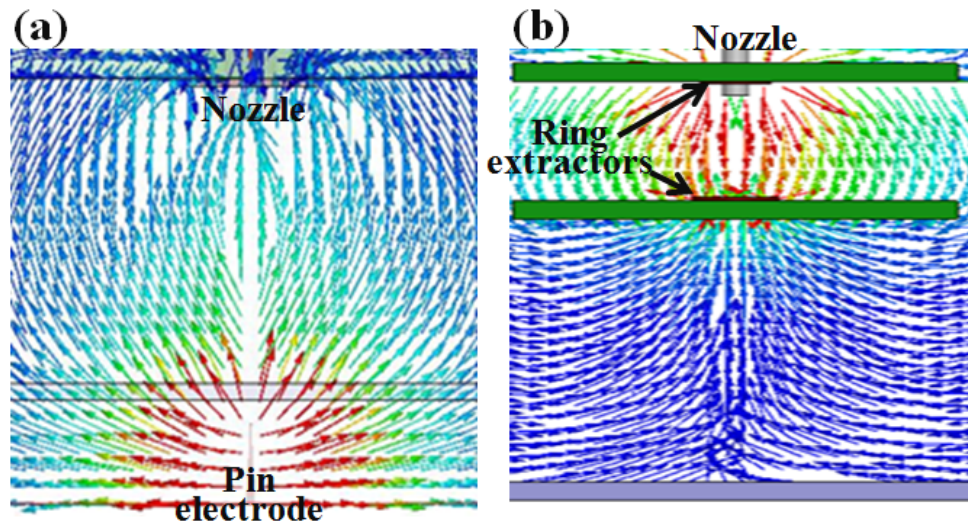


Figure 2.6 Electric field analysis of (a) pin electrode and (b) ring extractors.

2.3 Thermal bubble hybrid jetting system

2.3.1 Principle

Figure 2.7 shows the principle of operation of the thermal bubble HJS. In this system, when the driving waveform [figure 2.8] is applied to heater which inside the fabricated thermal jet head, this energy make nucleation in the heater. And, this nucleation makes the thermal bubble on the surface of the heater. The growing of the thermal bubble induce the changing pressure of inside chamber of fabricated thermal jet head. This changing deform the meniscus and extruded outside of the PCB nozzle of thermal jet head. Here, it is important to optimize the applied driving waveform and the back-pressure in accordance with the kind of liquid because large droplets are ejected by the excessive displacement of thermal jet head. In this state, when the electric potential is applied between PCB nozzle and pin electrode which located under substrate, the meniscus is changed into taylor cone. And ultra fine droplets are ejected at the end of taylor cone. When the driving waveform is turned off and the pressure inside the chamber of thermal jet head is decreased, the meniscus of the liquid returns to the initial position. Then, one cycle of the jetting is complete.

In contrast to the pulsed cone-jet mode (where the operational voltage is several kV), the shape of the liquid meniscus can be controlled through a thermal jet head. Using this principle, ultra-fine droplets can be generated with a high frequency of up to 1 kHz. Furthermore, the response characteristics of the HJS are better than those of the pulsed cone-jet and pulsating jet modes because the delay time for making a Taylor cone is negligibly small.

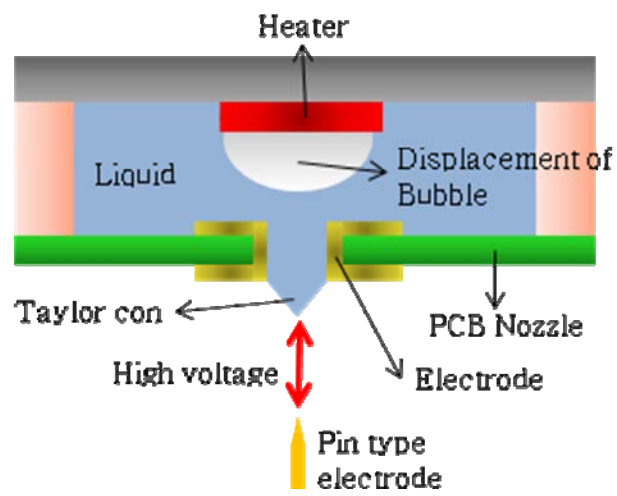


Figure 2.7 Principle of thermal bubble HJS

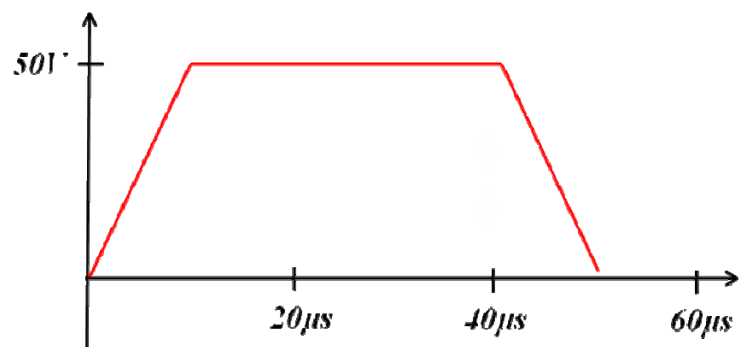


Figure 2.8 Driving waveform of thermal bubble HJS

2.3.2 Design & fabrication

Figure 2.9 shows the fabrication step of PCB based thermal jet head for applying multi nozzle hybrid jetting system. PCB based thermal jet head consists of bottom plate which is made by MEMS process and upper plate which is made by PCB process. By attaching the fabricated two plates, the thermal jet head is fabricated finally.

The fabrication steps of bottom plate are like this. (a) deposition of the barrier layer(SiO_2) on the silicon wafer, (b) deposition of the heater layer which consists Ti(10nm) and Pt(40nm) using the E-beam evaporator and patterning the heater, (c) deposition of the electrode layer which consists Ti(20nm) and Cu(200nm) using E-beam evaporator, (d) deposition of passivation layer (SiO_2) of 0.6 μm using LPCVD, (e) making the Su-8 (100) chamber of 150 μm and channel, (f) by attaching the fabricated heater plate to PCB nozzle, the thermal jet head is fabricated finally.

The fabrication steps of PCB nozzle plate are like this. (a) formation of nozzle holed (200 μm) using the drilling on the FR-4 substrate, (b) electroplating of Cu and patterning the electrode and wire, (c) deposition of SR for enhance the electrical isolation, (d) Teflon coating (AF2400, Dupont Corp).

The fabricated thermal jet head and PCB nozzle are shown in Figure 2.10.

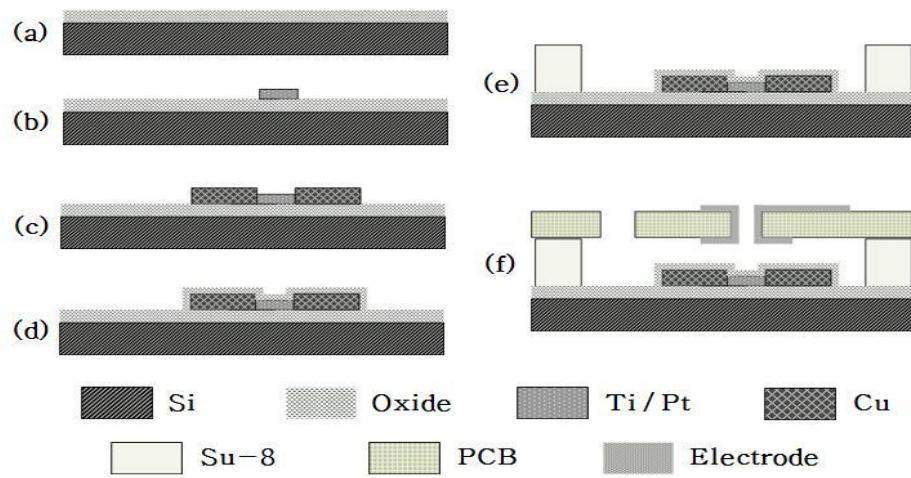


Figure 2.9 Fabrication steps of the thermal bubble HJS.

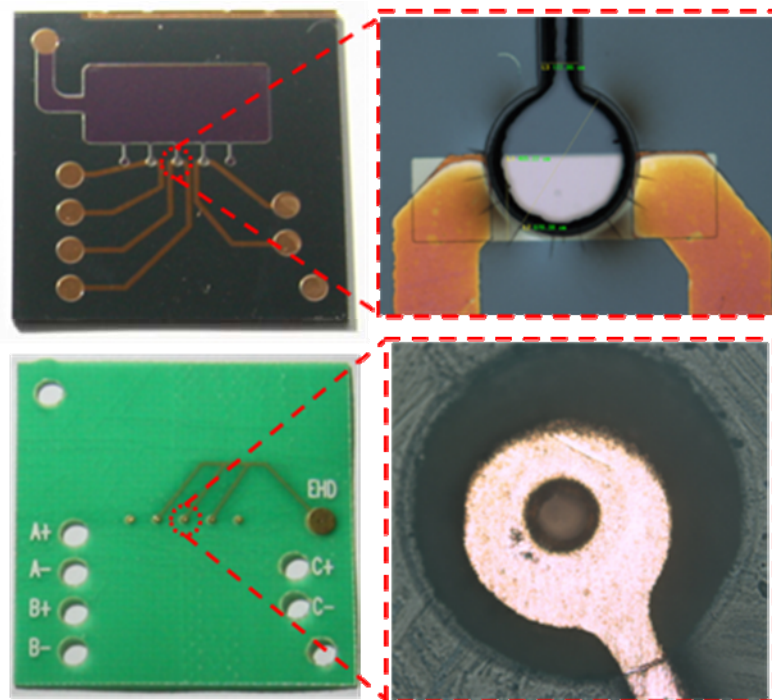


Figure 2.10 Fabricated thermal jet head and PCB nozzle.

III. EXPERIMENTAL AND RESULTS

3.1 Ring extractors integrated HJS

3.1.1 Experimental setup

Figure 3.1 shows the experimental setup of the ring extractors integrated HJS. A piezoelectric actuating head (Microfab, MJ-AT-01-50) controls the quantity of a revealed meniscus with high frequency. The ring extractors apply the electrostatic force for jetting or velocity control of droplets to a glass capillary (inner diameter: 60 μm , outer diameter: 300 μm). A driving waveform generator (Softmecha) makes a driving waveform that is applied to the piezoelectric actuator. A trigger source was used to synchronize the driving waveform and high speed camera. A power supply (HV-Rack, Ultravolt Inc.) generates a dc high voltage that is applied to the ring extractors. A pneumatic device (EFD-2400) maintains the initial vertical position and a uniform shape of the meniscus. A high speed camera (Motion pro HS-4, Redlake Inc.) and halogen light source (KLS-100H-RS-150) were used to observe the deformation of the liquid meniscus and the jetting of droplets. The liquid used in this study was 99.7% $\text{C}_2\text{H}_5\text{OH}$ [table 3.1].

3.1.2 Drop-on-demand jetting

3.1.2.1 Meniscus control using piezoelectric actuator

Figure 3.2 shows the DOD jetting result of the ring extractors integrated HJS. DOD jetting is controlled by two important input values that are a driving waveform of the piezoelectric actuator and the dc voltage of the ring extractors. The DOD jetting of EHD techniques require a long time (2.74 ms), so that meniscus for jetting is formed outside the nozzle. It was important to deform the meniscus to an appropriate position because the jetting was determined by the distance between the meniscus and the bottom electrode. The higher waveforms resulted in smaller gaps between the meniscus and the bottom electrode, and in larger droplet sizes. Also, these higher waveforms had an effect on the damping of the liquid meniscus (in the case of hybrid jetting with a waveform of -10 to 20 V, damping ended within $90\text{ }\mu\text{s}$). Therefore, for the optimal condition of the driving waveform, it was necessary to obtain better jetting properties, such as small droplet sizes and high jetting frequencies.

The Piezoelectric actuator uses a piezoelectricity material to achieve transformation at high speed via the driving waveform. As shown in Fig. 3.2, it can form meniscus for jetting in a short period of time ($\sim 30\text{ }\mu\text{s}$). To increase the hydrophobicity, the glass capillary was treated with Teflon (AF2400, DuPont Corp.). So, pulsation of the meniscus has the same size ($60\text{ }\mu\text{m}$) as the inner diameter of the glass capillary. Pulsation of the meniscus by applying the waveform was observed during $150\text{ }\mu\text{s}$, which is the minimum time for generating a stable droplet. Thus, by using the proposed printing system, high throughput jetting over 5 kHz can be operated

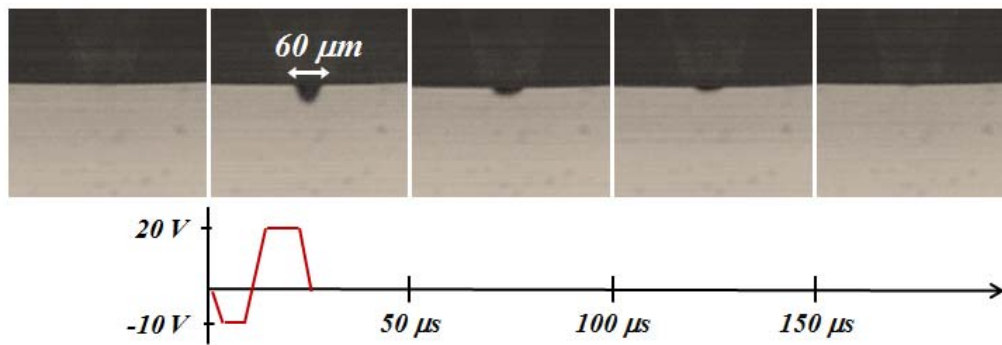


Figure 3.2 Detail meniscus control through a piezoelectric actuator. Pulsation continued until $150\ \mu\text{s}$ after the waveform applied.

3.1.2.2 Jetting of ultra fine droplets

Figure 3.3 shows that fine droplet jetting is achieved by applying the dc voltage to the ring extractors when meniscus is controlled by the piezoelectric actuator. It was possible to produce a liquid meniscus with a similar size to the inner diameter of the glass capillary (60 μm , treated with Teflon (AF2400, DuPont Corp.) to increase the hydrophobicity) and to form a Taylor cone of small volume. This was mainly due to the hydrophobic treatment of the capillary. Also, it was very important to precisely control the initial position of the liquid meniscus by the back-pressure through a pneumatic controller.

At 10 μs , the actuator was displaced and the inside pressure of the capillary was increased when the driving waveform was applied to the piezoelectric actuator. As a result, the liquid meniscus was extruded outside of the glass capillary. At 20 μs , the extruded meniscus was transformed into a conical shape by an existing high voltage and the ejection of the cone-jet commenced. Although the driving waveform was turned off at 30 μs , jetting did not finish but continued till 80 μs because of the inertia of the liquid and the residual electric force. At 90 μs , the whole jetting process fully finished and the meniscus returned to the initial position. This means that one jetting period could be finished within 90 μs and theoretically jetting with a frequency of about 1 kHz could be achieved.

During 20 μs to 40 μs , meniscus was changed to conical shape by the electrostatic field. At 60 μs , the droplet was perfectly ejected at apex of extruded meniscus. Through these mechanisms, ultra fine droplet was generated with high jetting frequency. The DC voltage applied to the ring extractor is 2.3 kV in comparison with

that of the previous HJS at ~5 kV [11]. The jetting frequency is 5 kHz. The volume of droplet can be estimated as $\pi \times 5 \mu\text{m}^2 \times 17 \mu\text{m} = 1.33 \text{ pl}$

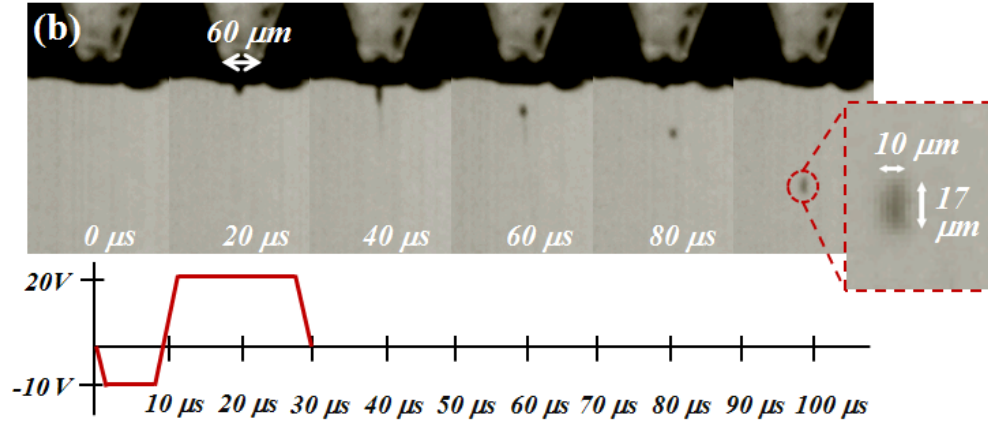


Figure 3.3 DOD ejection results using the proposed HPS. The Jetting cycle and droplet volume were under 100 μs and 1.33 pl.

3.1.3 Velocity control of droplets

3.1.3.1 Piezoelectric jetting in various driving waveform

The ring extractors integrated HJS achieves velocity control of the droplet as well as high frequency jetting of the fine droplet. First, to analyze effect that the driving waveform gives in the droplet velocity and size, a variable waveform with difference amplitude was used [Fig. 3.4(a)]. The velocity and size of droplets were estimated via a high speed camera. The jetting results were observed at fixed time after the driving waveform was applied to the piezoelectric actuator [Fig. 3.4(b): 100 μ s, Fig. 3.4(c): 300 μ s].

As shown in Fig. 3.4(b), the high waveform swelled the quantity of initial meniscus because it does greatly deform the piezoelectric material. This changes the droplet volume that becomes jetting. As shown in Fig. 3.4(c), the distance between the tip of the glass capillary and the droplet means that velocity is increased, but the size of the droplet is also increased. It means that the change of a driving waveform can control the droplet velocity, but it can also change the size of the droplet. Therefore, the technology that controls the droplet velocity without changing the driving waveform is necessary.

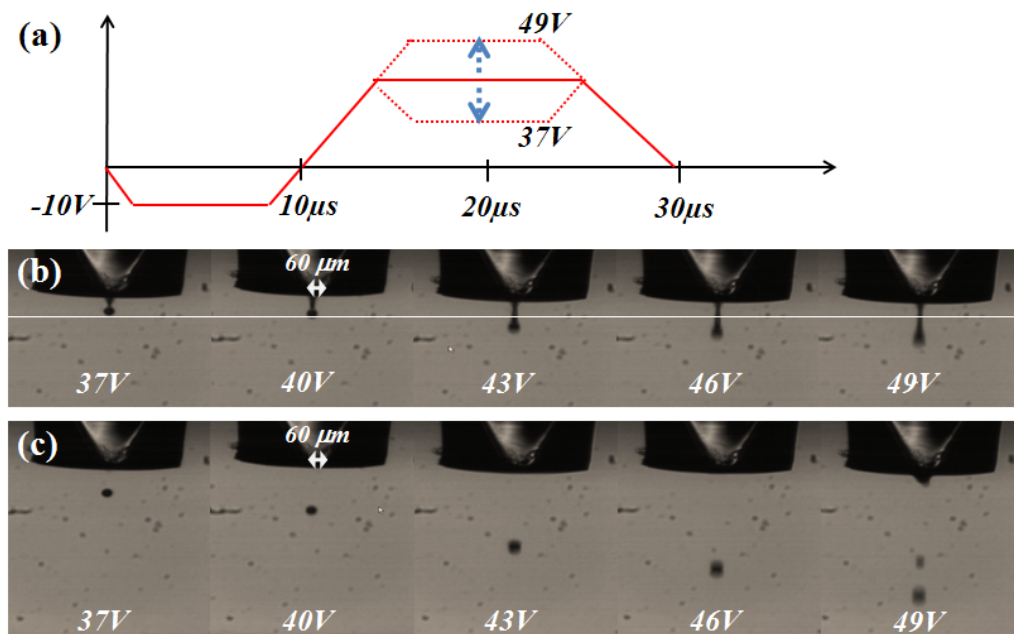


Figure 3.4 Jetting results of various driving waveform at (b) 100 μs and (c) 300 μs

3.1.3.2 Accelerated droplet in electrostatic field

Figure 3.5 shows the jetting of droplet in the electrostatic field that is applied by the ring extractors. In the fig. 3.5(a) the distance between glass capillary and tip of droplets was $46.6\text{ }\mu\text{m}$ but when the dc voltage was applied to ring extractors, the distance between glass capillary and tip of droplet was increased to $372.5\text{ }\mu\text{m}$

The form of droplets was also changed from spherical to stream shape as time went by ($100\text{ }\mu\text{s}$ ~ $300\text{ }\mu\text{s}$). The DC voltage to ring extractors was 1750V , and the driving waveform to piezoelectric actuator was 37V

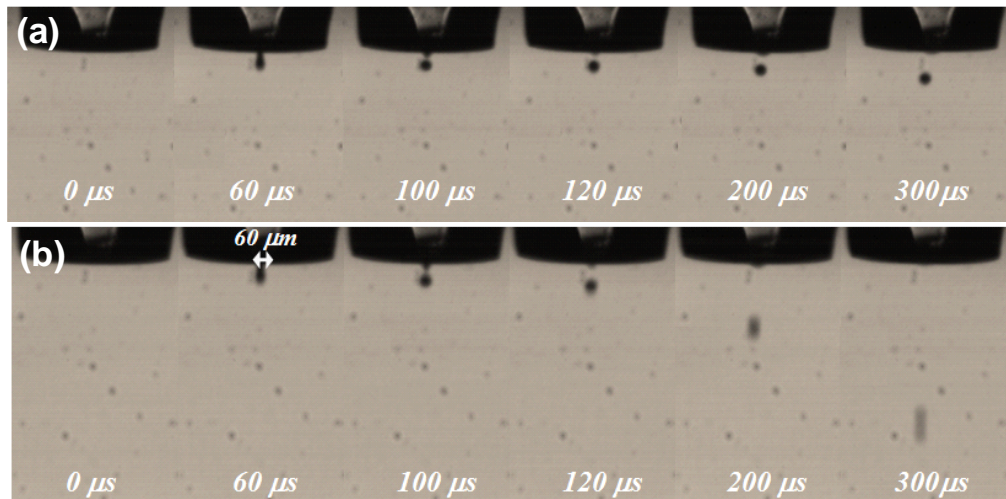


Figure 3.5 The jetting of droplet in the electrostatic field that is applied by the ring extractors

3.1.3.3 Drop velocity control using ring extractors integrated HJS

Figure 3.6(a) shows the jetting of droplet in the electrostatic field that is applied by the ring extractors. The form of droplets was changed from spherical to stream shape as time went by ($100\ \mu\text{s} \sim 300\ \mu\text{s}$). The DC voltage to ring extractors was 1750V, and the driving waveform to piezoelectric actuator was 37V. To demonstrate the effect of the DC voltage, various DC voltages ($500\text{V} \sim 1750\text{V}$) were applied on ring extractors at fixed waveform (37V) [Fig. 3.6(b), Fig. 3.6(c)]. The results were observed at fixed time after the driving waveform was applied to the piezoelectric actuator [Fig. 3.6(b): $100\ \mu\text{s}$, Fig. 3.6(c): $300\ \mu\text{s}$]. These values have low voltage to change the shape of meniscus. As shown in Fig. 3.6(b), the form of the initial meniscus was uniform because the driving waveform was fixed at 37V. As the applied DC voltage was higher, the dropping distance of a droplet from the nozzle increased. And when applying 1750V, the distance was 3 times longer than that when applying 250V.

It means that the volume of the ejected droplets is the same. The ejected droplet was accelerated by the electrostatic field that was formed on the ring extractors. So, we confirm that when a high DC voltage is applied, the distance between the glass capillary and the droplet increased

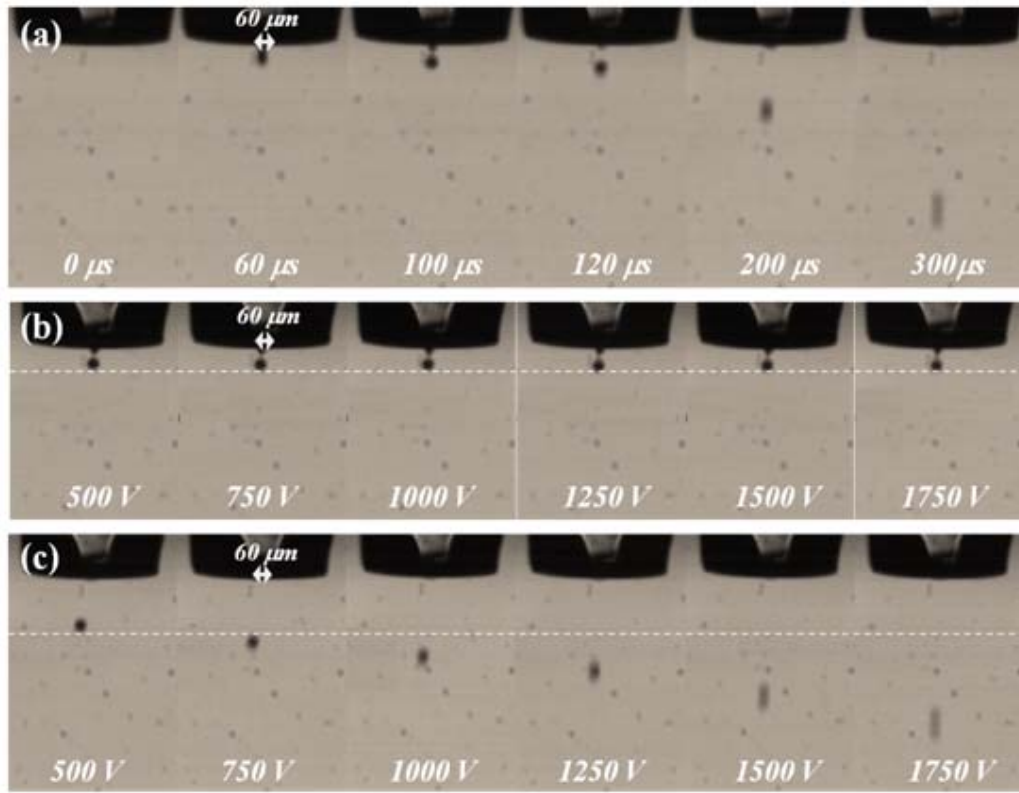


FIGURE 3.6 Velocity control of droplets using the ring extractors integrated HJS. (a) jetting characteristic in the electrostatic field, jetting results of various DC voltage at (b) 100 μs and (b) 300 μs, and

3.1.3.4 Calculated average droplet velocity

Table 3.2 show that the distance between the glass capillary and tip of droplets It was estimate by image of high speed camera. Applied voltage was 0 V to 1750 V. The distance was increased when higher dc voltage was applied.

Figure 3.7 shows that the average velocity ($v_{droplet}$) of the droplets between 100 μs and 300 μs in varying supplied DC voltages. It was calculated by

$$v_{droplet} = \frac{d_{300} - d_{100}}{300 - 100}$$

d_{100} : distance between the glass capillary and the droplets at 100 μs

d_{300} : distance between the glass capillary and the droplets at 300 μs

where d_{300} is the distance between the glass capillary and the droplet at 300 μs , and d_{100} is the distance between the glass capillary and the droplet at 100 μs . As the voltage increases, the velocity of droplets also increases. When applying 1750V, the velocity was 4 times faster than that when applying 500V. From these results, we could confirm that the velocity of the droplet could be controlled by DC voltage of ring extractors.

	500V	750V	1000V	1250V	1500V	1750V
d_{100}	46.6	46.6	46.6	46.6	46.6	46.6
d_{300}	122.5	161	207	242.5	310	372.5
$v_{droplet}$ (cm/s)	37.95	57.2	80.2	97.95	131.7	162.95

TABLE 3.2. THE DISTANCE BETWEEN THE GLASS CAPILLART AND TIP OF DROPLET

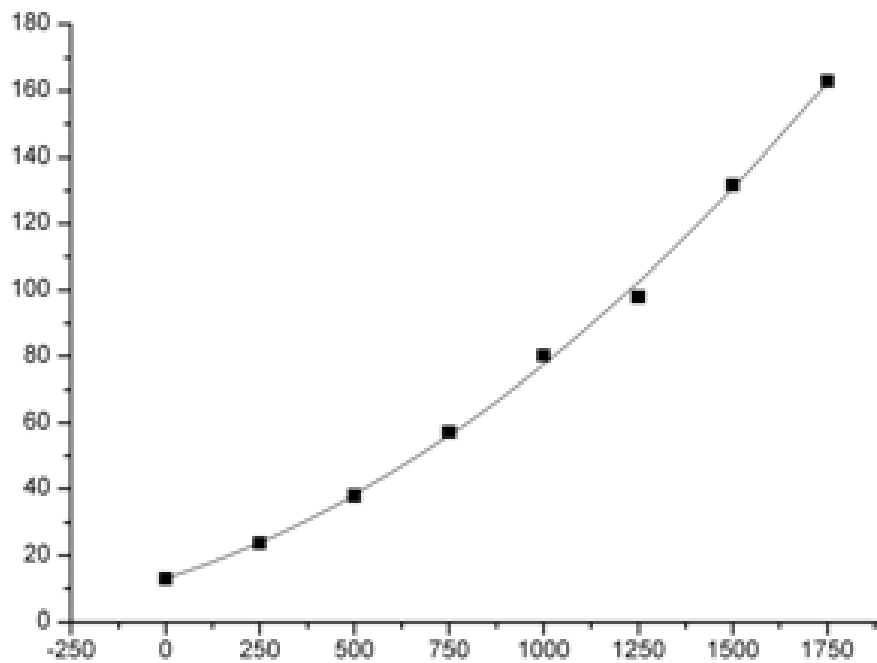


Figure 3.7 The average velocity ($v_{droplet}$) of the droplets between 100 μ s and 300 μ s
in varying supplied DC voltages

3.2 Thermal bubble hybrid jetting system

3.2.1 Experimental setup

Figure 3.8 shows the experimental setup of the thermal bubble HJS. The fabricated thermal jet head controls the quantity of a revealed meniscus with high frequency. the electro static force is applied between electrode of PCB nozzle and pin electrode under the substrate. A driving waveform generator (Softmecha) makes a driving waveform that is applied to the piezoelectric actuator. A trigger source was used to synchronize the driving waveform and high speed camera. A power supply (HV-Rack, Ultravolt Inc.) generates a dc high voltage that is applied to the ring extractors. A pneumatic device (EFD-2400) maintains the initial vertical position and a uniform shape of the meniscus. A high speed camera (Motion pro HS-4, Redlake Inc.) and halogen light source (KLS-100H-RS-150) were used to observe the deformation of the liquid meniscus and the jetting of droplets. The liquid used in this study was 99.7% C₂H₅OH [table 3.3].

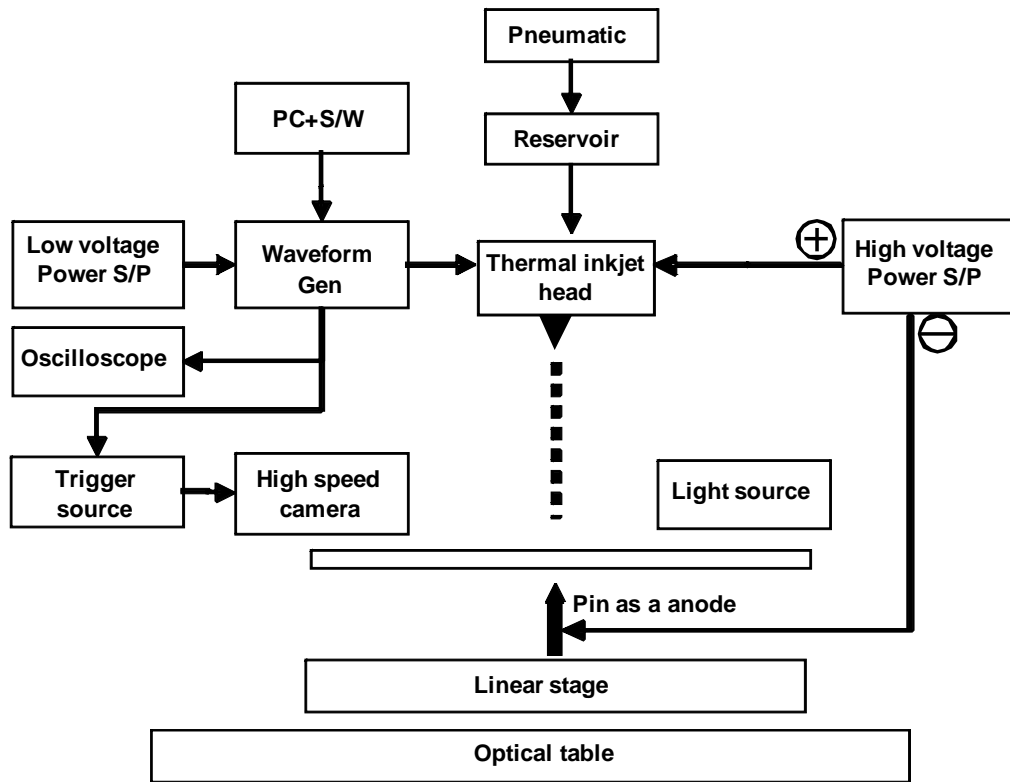


Figure 3.8 Experimental setup of thermal bubble HJS.

Viscosity (mPa s)	Electrical conductivity (S m ⁻¹)	Relative permittivity (ϵ_i/ϵ_0)	Surface tension coefficient, γ (N m ⁻¹)	Density (kg m ⁻³)	Charge relaxation time (s)
1.16	3.0×10^{-4}	25	0.022	789	6.0×10^{-7}

Table 3.3 Physical properties of the liquid used in the thermal bubble HJS.

3.2.2 Jetting results of fabricated thermal jet head

Figure 3.9 shows that jetting results of fabricated thermal jet head. It was observed by high speed camera. The initial meniscus was fixed by pneumatic device. It was very important to precisely control the initial position of the liquid meniscus by the back-pressure (0.6 kPa) through a pneumatic controller. And then, to make the bubble on the heater which located in the thermal jet head, driving waveform(40V, 50 μ s, 500Hz) was applied to the heater. It makes the changing of the pressure inside chamber. As a result, the liquid meniscus was ejected outside of the PCB multi nozzle. For hydrophobic property, the PCB nozzle was coated by Teflon (AF2400, DuPont Corp.).

We demonstrated the drop-on-demand characteristic of thermal jet head. The droplet was perfectly ejected by driving waveform which is applied to the heater. As shown in figure 3.9, there are satellite droplets. For reducing this phenomenon, it is important to optimize the driving waveform and initial pressure of the chamber.

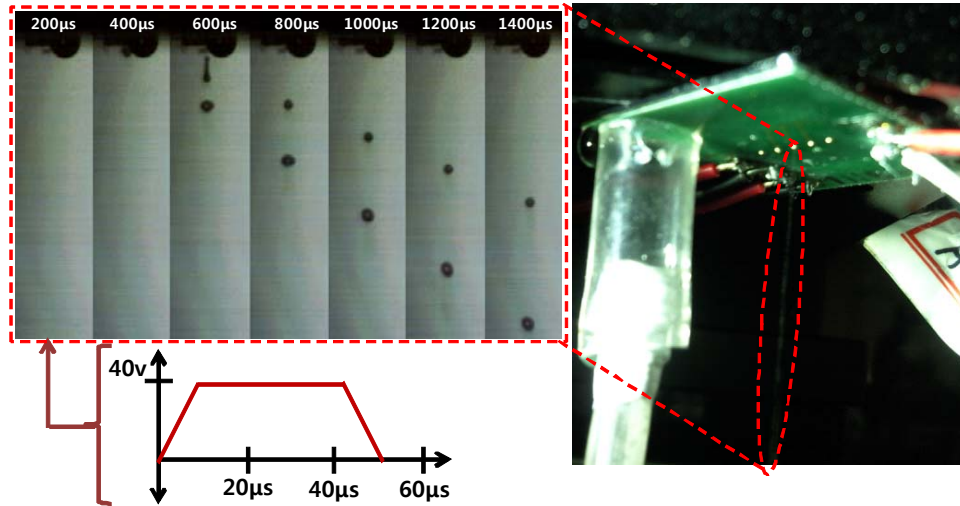


Figure 3.9 Drop-on-demand jetting result of the fabricated thermal jet head.

IV. Conclusion

4.1 Summary

We have demonstrated two types of hybrid jetting system, termed ring extractor integrated HJS and thermal bubble HJS.

Ring extractors integrated hybrid jetting system (HJS) solves the problems of pin electrode of previous HJS. Ring extractors can apply electrostatic force to nozzle without substrate effect. The proposed HJS is capable of:

(1) generating ultra-fine droplets through an extremely short duration of the driving waveform (one droplet generation cycle is $90\ \mu\text{s}$), in comparison with existing methods (the time for one droplet-generation cycle of the pulsating jet mode is 3–10 ms and the delay time of the pulsed cone-jet mode is 3.6 ms), (2) modulating the size of droplets by controlling the duration and the magnitude of the driving waveform and (3) high-frequency operation up to 1 kHz.

In conclusion, the ring extractor integrated HJS has unique features as follows. First, we can simultaneously achieve both ultra-fine droplets and jetting on demand with high frequency. This is a unique feature of the proposed ring extractor integrated HJS in comparison with conventional inkjet printing and EHD jetting techniques. Second, ultra-fine droplets were generated through mechanical actuation and not high-voltage pulses that are widely used in drop-on-demand EHD jetting. This system also capable of control the droplet velocity in the piezoelectric actuating mode. The droplets are generated by fixed driving waveform. So, excluded volume of ink is same in the variable dc voltage of ring extractors. But, flight droplets are influenced

by electrostatic field which formed in ring extractors. This force can control the droplet velocity. It can contribute to reduce velocity deviation of droplets in multi-nozzle jetting systems without changing volume of droplets.

For multi nozzle HJS, we made thermal inkjet head. It was consist of heater plate which was made by MEMS process and nozzle plate which was made by PCB process. By using PCB nozzle, we improved the electrical insulating properties of nozzle surface and reduced fabrication cost. Using this multi nozzle hybrid jetting head, we could control the meniscus and eject droplets with frequency of 500Hz.

REFERENCE

- [1] Douglas B. Chrisey, “MATERIAL PROCESSING: The Power of Direct Writing”, *Science*, Vol. 289, pp. 879 ~881, 2000

- [2] Tao Xu, Cassie A. Gregory, Peter Molnar, Xiaofeng Cui, Sahil Jalota, Sarit B. Bhaduri and Thomas Boland, “Viability and electrophysiology of neural cell structures generated by the inkjet printing method”, *Biomaterials*. Vol. 27, pp. 3580~3588, 2006

- [3] Hak Sung Kim, Jin Sung Kang, Jong Se Park, H. Thomas Hahn and Jae Woo Joung, “Inkjet printed electronics for multifunctional composite structure”, *Compos. Sci. Technol.* Vol. 69, pp. 1256~1264, 2009

- [4] Vinay J. Nagaraj, Seron Eaton, Derek Thirstrup, Peter Wiktor, “ Piezoelectric printing and probing of lectin nanoprobearrays for glycosylation analysis”, *Biochemical and Biophysical Research Communications*, Vol. 375, pp. 426-430, 2008

- [5] Ki Deok Bae, Seog Soon Baek, Hyung Taek Lim, Keon Kuk, Kwang Choon Ro, “ Development of the new thermal inkjet head on SOI wafer”, *Microelectronic Engineering*, Vol. 78-79, pp. 158-163, 2005

- [6] Yogi O, Kawakami T, Yamauchi M, Ye J Y and Ishikawa M, “ On-demand droplet spotter for preparing pico- to femtoliter droplets on surfaces”, *Anal. Chem.*, Vol. 73, pp. 1896~1902, 2001

- [7] Alvin U. Chen and Osman A. Basaran, “ A new method for significantly reducing drop radius in drop-on-demand drop production”, *PHYS. FLUIDS*, Vol. 14, pp. L1~L4, 2002

- [8] Joonghyuk Kim, Hyuncheol Oh and Sang Soo Kim, “ Electrohydrodynamic drop-on-demand patterning in pulsed cone-jet mode at various frequencies”, *Aerosol Science*, Vol. 39, pp. 819-825, 2008.

- [9] H.F. Poon, Ph.D., “Electrohydrodynamic Printing”, thesis, Princeton University, 2002

- [10] C.-H. Chen, D. A. Saville, and I. A. Aksay, “Scaling laws for pulsed electrohydrodynamic drop formation”, *Appl. Phys. Lett.* Vol. 89, PP. 124103, 2006

- [11] Young-Jae Kim, Sang-Yoon Kim, Jun-Sung Lee, Jungho Hwang and Yong-Jun Kim, “On-demand electrohydrodynamic jetting with meniscus control by a piezoelectric actuator for ultra-fine patterns”, *J. Micromech. Microeng.* Vol. 19, pp. 107001, 2009

- [12] A. Jaworek and A. krupa, "Classsification of the modes of EHD spraying", J. Aerosol Sci. Vol. 30, pp. 975, 1999

- [13] Sung-Jun Pak, Shanghoon Seo and Jaewoo Joung, "Fine micro patterning of conductive line by using direct inkjet printing", KEM. Vol. 326, pp. 257~260, 2006

- [14] Hongming Dong, Wallace W. Carr and Jeffrey F. Morris, "An experimental study of drop-on-demand drop formation", Phys. Fluids. Vol. 18, pp. 072102, 2006.

- [15] D. Y. Lee, Y. S. Shin, S. E. Park, T. U. yu, and J. Hwang, "Electrohydrodynamic printing of silver nanoparticles by using a focused nanocolloid jet", J.Appl. Phys. Lett., Vol.90, 081905, 2007

- [16] J. L. Li, "EHD spraying induced by the pulsed voltage superimposed to a bias voltage", J. Elec., Vol. 65, pp. 750-757, 2007

- [17] J. D. Regele et al., "Effects of capillary spacing on EHD spraying from an array of cone jets", J. Aerosol Sci., Vol. 33, pp. 1471-1479, 2002

- [18] Jaeyong Choi, Yong-jae Kim, Sukhan Lee, Sang Uk Son, Han Seo Ko, Vu Dat Nguyen and Doyong Byun, “Drop-on-demand printing of conductive ink by electrostatic field induced inkjet head”, *Appl. Phys. Lett.* Vol. 93, pp. 193508, 2008.

- [19] Sukhan Lee, Doyoung Byun, Daewon Jung, Jaeyong Choi, Yongjae Kim, Ji Hye Yang, Sang Uk Son, Si Bui Quang Tran and Han seo Ko, “Pole-type ground electrode in nozzle for electrostatic field induced drop-on-demand inkjet head”, *Sens. Actuators, A* Vol. 141, pp. 506~514, 2008.